model a complete description of a heteropolysaccharide ether requires the mole fractions of the monosaccharide types comprising the original polymer and a set of relative rate constants of reaction of the hydroxyls. There is a degree of chemical selectivity in the reactivity of the different hydroxyls of guar (see Table II). The primary hydroxyls at positions 6 of mannose and galactose are preferred in the hydroxypropylation reaction, the sequence being $k_{M6} \simeq k_{G6} > k_{M'2} \simeq k_{M2} > k_{G3} \simeq k_{M3} \simeq k_{M'3} \simeq k_{G2} > k_{G4}$. On the other hand, in the carboxymethylation reaction there is a slight preference for position 2 of mannose, the sequence being $k_{M2} \simeq k_{M'2} \simeq k_{M6} > k_{G6} > k_{G2} > k_{G3} \simeq k_{G4} > k_{M'3} \simeq k_{M3}$. Similar trends can be observed in comparing (hydroxyethyl)cellulose[6] and (carboxymethyl)cellulose.[5] Note that the involvement of carbon 6 of mannose in the glycosidic linkage with galactose has only a minor influence on the relative reactivities of the hydroxyls at positions 2 and 3. Thus, the assumption that substitution within a given unit does not affect the reactivity of the remaining hydroxyls receives independent support.

References and Notes

(1) Seaman, J. K. In "Handbook of Water-Soluble Gums and Resins"; Davidson, R. L., Ed.; McGraw-Hill: New York, 1980; Chapter 6.
(2) McNeil, M.; Albersheim, P. *Carbohydr. Res.* **1984**, *131*, 131.
(3) McNeil, M.; Szalecki,, W.; Albersheim, P. *Carbohydr. Res.* **1984**, *131*, 139.
(4) Spurlin, H. M. *J. Am. Chem. Soc.* **1939**, *61*, 2222.
(5) Reuben, J.; Conner, H. T. *Carbohydr. Res.* **1983**, *115*, 1.
(6) Reuben, J. *Macromolecules* **1984**, *17*, 156.
(7) Wu, T. K. *Macromolecules* **1980**, *13*, 74.
(8) Also, these expectation values provide a mathematical means of resolving pairs of monomers that could not be separated chromatographically.

Structural Changes in Polystyrene–Polybutadiene–Polystyrene Block Polymers Caused by Annealing in Highly Oriented State

Tadeusz Pakuła,† Kenji Saijo, and Takeji Hashimoto*

Department of Polymer Chemistry, Faculty of Engineering, Kyoto University, Kyoto 606, Japan.

Received October 2, 1984

ABSTRACT: The effect of annealing on morphological changes of highly oriented SBS block polymers was studied by small-angle X-ray scattering techniques. The SBS block polymer specimens studied had a morphology of cylindrical microdomains of polystyrene (PS) in a matrix of polybutadiene in the undeformed state. They were deformed initially to a draw ratio of $\lambda_0 = 6$ and then annealed at constant dimensions at various temperatures between 50 and 250 °C. Depending on the annealing temperature T_a, various morphological changes were observed: (i) at $T_a < T_g$ (the glass transition temperature of PS), the resultant morphology was influenced by both nonrecoverable reorientation of the microdomains and elastically recoverable orientation; (ii) at $T_g < T_a < T_c$ (order–disorder transition of the block polymer), well-oriented microdomain morphology was formed by nonrecoverable reorientation of polystyrene microdomain; and (iii) at $T_a > T_c$, morphology of the cylindrical microdomains with macroscopically random orientation was re-formed from the block polymers in disordered state. Molecular interpretations of observed morphological changes were presented. Residual deformation in bulk specimens and anomalous behavior of birefringence of the specimens with annealing temperature were interpreted phenomenologically on the basis of a "two-state" model.

I. Introduction

Polystyrene–polybutadiene–polystyrene (SBS) block polymers having a domain structure of alternating lamellar or of cylindrical microdomains of polystyrene (PS) component in the matrix of polybutadiene (PB) behave initially as a plastic material when stretched at temperatures below the glass-transition temperature (T_g) of PS. However, when they are stretched beyond the yield point they become rubbery, with high elasticity and large elastic deformation.[1-5] This is a phenomenon known as "strain-induced plastic-to-rubber transition". It is believed that the yielding process involves fragmentation of the original glassy domains that, even being fragmented, preserve properties of glassy material and play the roles of physical cross-links and fillers for the highly stretched rubbery matrix.[6,7] It was also observed that after the sample was stretched and the external stress removed, the sample recovers to almost its original length, and the structure can heal to the original one by annealing even at temperatures below T_g of PS.[2-4]

There are, however, no systematic researches about structural changes and relaxations induced by heat treatments in the deformed state. It is expected that the stretched samples of SBS block polymers will break up when heated above T_g because above the T_g the polystyrene domains cannot resist stresses exerted by highly stretched polybutadiene parts of molecules. This is probably why the thermally induced morphological changes in oriented block polymers have not been studied so far at temperatures above the glass transition. In order to circumvent this difficulty we used a special method that ensures constant dimensions of samples and does not involve sample breakage during annealing. The test specimens used in this work are SBS block polymers having the morphology of cylindrical PS domains in a matrix of PB in undeformed state. The deformation mechanism of these samples was systematically studied in our previous paper.[6]

Studies on thermally induced morphological changes and relaxations of block polymers, while keeping their bulk dimension constant, may have the following scientific and practical significance. (i) They should lead to molecular understandings of the domain–deformation mechanism and structural and molecular relaxations (i.e., "self-organization"[16]) processes. (ii) They should also provide fundamental information in regard to control of domain orientation. The highly stretched block polymers have the particular morphology and orientation of domains described in detail in our previous work.[6] Questions will

†On leave from the Center of Molecular and Macromolecular Studies, Polish Academy of Sciences, Łodz, Poland. Present address: Max-Planck-Institut für Polymer Forschung, Mainz, W. Germany.

0024-9297/85/2218-2037$01.50/0

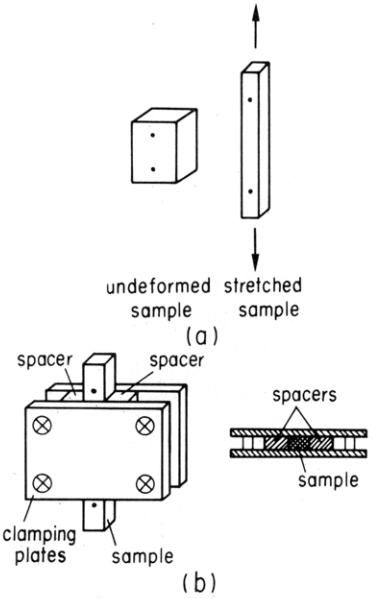

Figure 1. Sample holder for annealing of drawn samples in extended state.

naturally be raised as to whether or not one can fix and control the particular orientation of domains by heat setting. A particularly interesting orientation of the domains that has not been realized so far is uniaxial orientation of the cylindrical domains with respect to the stretching direction (SD), with the cylindrical axes normal to SD. This orientation, however, turns out to be unattainable by the method employed in this study due to the molecular relaxation process and plastic flow mechanism, as depicted in Figure 6 (see sections III-4 and IV).

As a byproduct of this research we found a quick method to estimate the order–disorder transition of block polymers based on birefringence measurements of the stretched samples as a function annealing temperature (see section III-5).

II. Experimental Methods

Two polymers studied in the former paper[6] have been used also in this work: (1) SBS block polymer designated TR 41-1648 (Shell Development Co.) with 29.3% polystyrene and total molecular weight M_v = 110 000 and (2) SBS block polymer designated TR 1102 (Shell Development Co.) with 28% polystyrene and molecular weight M_n = 52 000 and M_w = 76 000 (measured from GPC). Film samples were obtained by solvent casting from 10% solution of the polymer in toluene. Specimens in the form of ribbons cut from films were stretched by a hand-driven stretching device. The extension was measured by the distance between the marks on the film surface.

Figure 1 illustrates schematically changes of the sample dimensions caused by stretching (a) and also the device by which the dimensions of stretched samples were kept constant after removal of the external stretching force (b). The device consists of two metal plates and two spacers. The thickness of the spacers was in all cases adjusted to be equal to the thickness of the deformed sample. Two spacers were clamped by parallel plates in such a way that the space between them had the shape and dimensions as close as possible to the shape of the deformed sample. The removal of the external stretching force caused the recovery of nonclamped parts of the sample, but the clamped part was proven to preserve the same dimensions as it had under extensional force. In fact, this part of the sample comes to be under pressure (not under tension), but it is believed to preserve the orientation and structure produced by stretching.

The samples were first drawn to extension ratio $\lambda_0 = 6$, clamped with the device described above, and then subjected to annealing in the deformed state at various temperatures for the same period of time, t_a = 30 min unless otherwise stated, in order to investigate

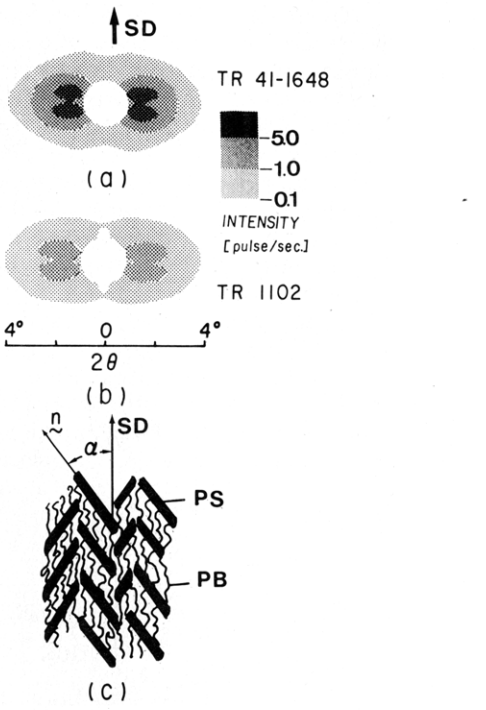

Figure 2. SAXS patterns of samples deformed to $\lambda_0 = 6$: (a) TR 41-1648, (b) TR 1102. (c) Schematic representation of related microdomain structure.

the effect of annealing temperature T_a. The heating and cooling rates were not controlled precisely, but they were rather high in comparison with t_a^{-1}. After the samples were annealed at T_a for t_a, they were cooled to room temperature and taken from the holding device. The samples were then subjected to measurements of bulk dimensions, birefringence, and small-angle X-ray scattering (SAXS) at room temperature.

The birefringence of samples was measured by using a polarizing microscope with Berek compensator. Two-dimensional SAXS patterns were obtained by using the rapid detection system with rotating anode X-ray generator and a position-sensitive proportional counter (PSPC), which was described in detail in other papers.[6,8,9] In experiments reported here the pinhole collimation was used with two pinholes of 0.5-mm diameter at a distance of 400 mm in the path of incident beam axis and with the slit height-limiting device in front of the PSPC. The scattered X-ray intensity distributions with the scattering angle 2θ were detected with one-dimensional PSPC set along the horizontal direction at a distance of 1154 mm from the sample. Intensity distributions with azimuthal angle were measured by changing the stretching direction of the samples around incident beam axis. The intensity was corrected for absorption, air scattering, and background scattering and was used for construction of two-dimensional scattering patterns as shown in Figures 2, 5, and 8.

It should be noted that these SAXS patterns are not mere schematic illustrations, but rather the measured intensity distributions were quantitatively presented by three contour lines of equal intensity with 5, 1, and 0.1 pulses per second (in relative intensity levels) as shown in Figure 2. The same contour lines were used for all the figures in order to facilitate the comparisons. For convenience, to show the intensity distributions better, especially intensity increase and decrease, the scattered intensity distributions were divided into four regions with these three contour lines as the border lines.

III. Results and Discussions

1. Morphology of As-Drawn Samples. We describe here the morphology of starting materials that were drawn by extension ratio of $\lambda_0 = 6$ and used for further annealing experiments. The drawn samples were prepared from isotropic film specimens cast from toluene solution. The morphological changes involved by the large deformation were presented in detail in the previous paper.[6] Parts a

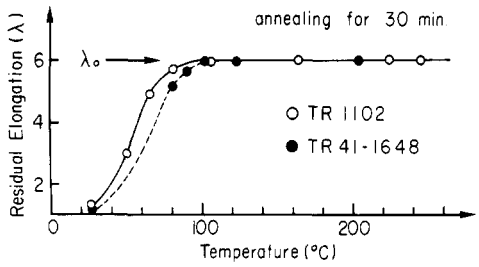

Figure 3. Dependence of residual elongation of macroscopically relaxed samples on annealing temperature. λ_0 is initial draw ratio.

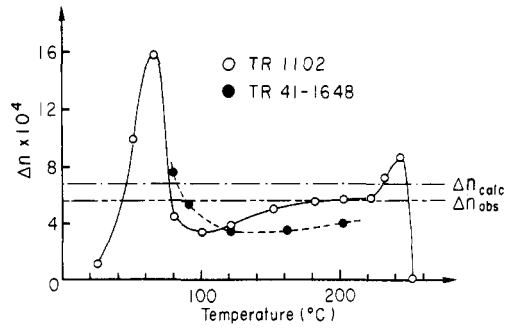

Figure 4. Dependence of residual birefringence of macroscopically relaxed samples on annealing temperature. Δn_{calcd} is the calculated form birefringence for perfectly oriented cylindrical microdomains and Δn_{obsd} is the observed birefringence for highly oriented cylindrical microdomains.

and b of Figure 2 show the SAXS patterns for the two kinds of SBS samples subjected to drawing of $\lambda_0 = 6$, and part c shows a schematic diagram for the morphology in the deformed state as predicted from the SAXS patterns.[6]

Such structure as shown in Figure 2c was concluded on the basis of consideration of two factors influencing the shape of the SAXS patterns, one related to the scattering from the single rodlike particle (particle factor) and the other related to the effect of the lattice that the particles can form (lattice factor). We refer to these results here because a sample deformed to $\lambda_0 = 6$ was in most cases a starting sample for further annealing experiments. It was found that at these large deformations the molecular orientation primarily controls the structure of samples.[6] The polybutadiene block chains are highly stretched and well oriented along the deformation direction (Figure 2c). The domain structure of the samples is, however, preserved, and the PS domains are spatially arranged with their centers along the drawing direction, but their longitudinal axes of the cylinders **n** are preferentially oriented along directions slightly inclined (by the angle α) to the drawing direction.

2. Residual Deformation. It was observed that some samples changed their dimensions after they were removed from the holder. The residual draw ratio λ as a function of annealing temperature is shown in Figure 3. It is seen that for samples annealed below T_g of PS domains there remains a certain portion of recoverable deformation which decreases, however, to zero upon increasing T_a toward T_g. For samples annealed at and above 100 °C, λ becomes equal to the initial draw ratio λ_0, suggesting that at these temperatures all stresses applied to the sample by stretching are relaxed during annealing.

3. Residual Birefringence—Form vs. Orientational Birefringence. Figure 4 shows the residual birefringence Δn as a function of T_a. The birefringence initially increases considerably but drops sharply with a further increase of T_a and reaches a minimum at T_g. Upon further increase of T_a it increases slightly again and reaches a plateau over a wide temperature range. Above 240 °C the birefringence drops again suddenly, indicating that samples annealed above this temperature become optically isotropic.

In the systems under consideration the net birefringence may be composed of two contributions: form birefringence caused by orientation of domains having a refractive index different from that of the matrix[10] and molecular birefringence caused by molecular orientation in both phases. The form birefringence for the system with perfectly oriented cylindrical domain morphology is given by Wiener's theory.[10]

$$\Delta n_{calcd} = \frac{v_1 v_2 (n_1^2 - n_2^2)^2}{2n_0[(v_1 + 1)n_2^2 + v_2 n_1^2]}$$

By assuming values $v_1 = 0.29$ and $v_2 = 0.71$ for volume fractions and $n_1 = 1.58$ and $n_2 = 1.52$ for the refractive indices of PS and PB phases, respectively, we obtain $\Delta n_{calcd} = 6.81 \times 10^{-4}$. The mean value of the refractive index (n_0) was assumed to be $n_0 = n_1 v_1 + n_2 v_2$. The calculated value was slightly higher than the birefringence $\Delta n_{obsd} = 5.6 \times 10^{-4}$ observed for samples of TR 1102 in which macroscopic orientation of the domains was obtained due to polymer flow during press-molding of samples.[6] Both of these values are shown in Figure 4 by means of horizontal dash–dot lines. It is seen that the maximum value of birefringence observed for samples of TR 1102 annealed below T_g in oriented state is much higher than the calculated form birefringence, Δn_{calcd}, and the measured birefringence, Δn_{obsd}. This means that the molecular orientation contributes significantly to the birefringences of samples annealed at these temperature, much more than the form birefringence. Above the glass-transition temperature, however, this orientational birefringence seems to become small because of stress relaxation and orientation relaxation of the system associated with the flow of PS domains, and hence the observed birefringence Δn is contributed to mainly by the form birefringence, as supported by the experimental evidence that the residual birefringence at the plateau region in $160 < T_a < 220$ °C is almost equal to Δn_{obsd}.

4. Morphological Changes upon Annealing As Observed by SAXS. Figure 5 shows typical changes of SAXS patterns for TR 1102 upon annealing at various temperatures. The behaviors of TR 41-1648 are not shown here because they are essentially identical with those of TR 1102. The changes of the four-point pattern observed for as-stretched samples (Figure 2) by annealing at a temperature T_a lower than the T_g of PS microphase indicate reorientation of the cylindrical microdomains involved by elastic recovery of samples (see structural change from Figure 6a,b). The reorientation due to elastic recovery is consistent with the observed residual draw ratios which are much smaller than λ_0 (Figure 3). At $T_a \ll T_g$, the reorientation involves a trend of re-formation of unoriented and undeformed microdomain structure. With increasing T_a toward T_g, the reorientation due to elastic recovery becomes less important, but the reorientation due to plastic flow of the polystyrene phase becomes increasingly important. The pattern obtained at $T_a = 50$ °C is already subjected to the flow effect to some extent. The latter reorientation mechanism will be described below.

At $T_a < T_g$ (e.g., $T_a \simeq 80$ °C; cf. Figure 11b), the stress is partially relaxed by the elastic recovery, the process of which invokes a tendency toward re-formation of unoriented and undeformed microdomain structures existing in the original solvent-cast film. The stress is partially relaxed also by plastic flow of polystyrene domains, the process of which causes orientational relaxation of polybutadiene chains and orientation of the polystyrene mi-

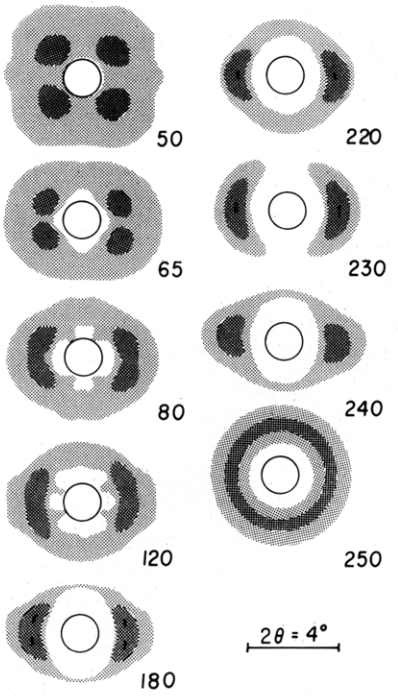

Figure 5. SAXS patterns for samples of TR 1102 annealed at temperatures indicated by the figures beside each pattern.

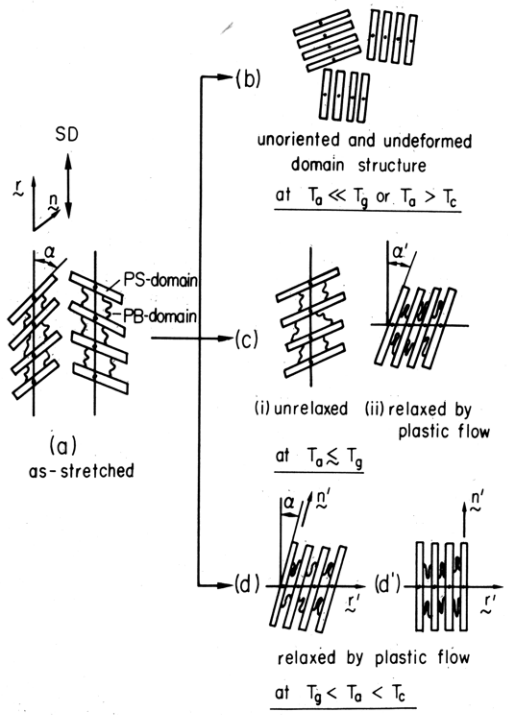

Figure 6. Schematic representation of structural changes caused by annealing at various temperatures and at constant deformation: (a) as-stretched before annealing; (b) after annealing either at $T_a \ll T_g$ or at $T_a > T_c$ (T_a, T_g, and T_c being the annealing temperature, the glass-transition temperature of polystyrene microdomains, and the order–disorder transition temperature of the block polymer, respectively); (c) after annealing at $T_a < T_g$; (d), (d′) after annealing at $T_g < T_a < T_c$.

crodomain toward the drawing direction, as indicated by the change of α to α' ($\alpha > \alpha'$) in Figure 6c. The latter process is responsible for the residual elongation after annealing, as shown in Figure 3, while the former process is responsible for the recoverable elongation. In Figure 6c, the states i and ii correspond to the states A and B in Figure 10a, respectively, as will be discussed in detail in section V. The coexistence of the "two states", corresponding to those unrelaxed and relaxed by the plastic flow, causes a partial orientation of the microdomains after annealing, as characterized by broader orientation distributions of the domain **n**′ and of the interdomain lattice vector **r**′ (see the patterns for 50–80 °C in Figure 5) compared with the corresponding orientation distributions before annealing.

At $T_a > T_g$, the SAXS patterns change their orientation, their intensity maximum being shifted from meridional to equatorial direction, indicating that the interdomain correlation changes its direction from **r** to **r**′, as shown in the schematically drawn structural change from Figure 6a to 6d or 6d′. The polystyrene domains having correlated interdomain distance along the drawing direction in the as-stretched, nonannealed specimens become correlated along the direction perpendicular to the deformation direction upon annealing above T_g. The orientation of the microdomains **n**′ in annealed samples is almost the same as or slightly more oriented toward SD than in the samples before annealing. At temperatures where the residual birefringence reaches the plateau in Figure 4, the SAXS patterns become two-point patterns with the maximum intensity at the equator, indicating that the microdomains assume orientation parallel to the direction of initial drawing (Figure 6d′).

5. Annealing Effect at High Temperature—Dissolution of Microdomains. For samples annealed above T_c the SAXS patterns do not indicate any orientation of the domains, as seen in Figure 5 for the pattern observed upon annealing at 250 °C. Here T_c may correspond to the order–disorder transition temperature of block polymers.[11-15,17] Above T_c the block polymers are in disordered state; the microdomain structure is thermodynamically unstable and is dissolved into a homogeneous mixture of PS and PB block chains. Below T_c the block polymers are in ordered state; the microdomain structures are thermodynamically stable. Consequently, upon annealing at $T_a > T_c$ the original microdomain structure is dissolved into a homogeneous mixture, and new microdomain structure with macroscopically random orientation is re-formed from the relaxed homogeneous mixture of the block chains when the sample is cooled below T_c. The sudden drop of birefringence at 250 °C, as shown in Figure 4, and circularly symmetric SAXS pattern at 250 °C, as shown in Figure 5, suggest that T_c for TR 1102 is about 250 °C.

Consequently, the birefringence method is proposed to be a useful, relatively easy, and quick method in the studies of the order–disorder transitions for SBS block polymers that give rise to the morphology with nonzero form birefringence.

6. Effect of Annealing Time. The effect of annealing time on the structural changes has not been studied in detail so far. In order to obtain some information on whether the observed structural states after the annealing are close to or far from equilibrium, we have measured dimensional and birefringence changes with annealing time for samples annealed at the lower annealing temperature of 50 °C. Results are shown in Figure 7 for samples drawn to various draw ratios. It is seen that the residual deformation and residual birefringence change quickly at short annealing time, but the changes slow down later and both quantities probably reach a plateau at a time longer than 1 h. The values of residual extension and birefringence observed after annealing for 0.5 h are close to the plateau values at all temperatures. It is reasonable to suppose that at higher temperatures the equilibrium states are reached at a shorter time of annealing.

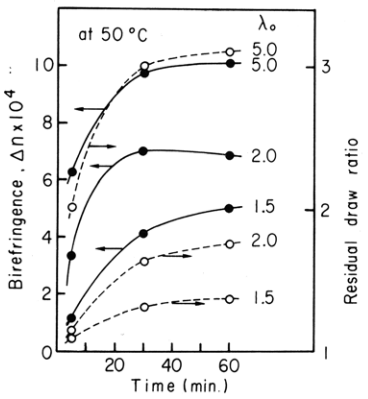

Figure 7. Residual birefringence and residual draw ratio vs. annealing time for samples deformed to various initial draw ratios λ_0 and annealed at 50 °C.

7. Effect of Heating and Cooling Rates. The effect of heating rate on the structure of annealed samples was observed for two specimens of TR 41-1643 drawn to λ_0 = 6 and heated to the same annealing temperature with different heating rates. The heating rate of the first sample was determined by heat conduction of the polymer when the sample was placed in the oven controlled at the temperature of annealing (T_a = 160 °C). The mean heating rate is estimated to be of the order of 100 °C/min. The other sample was heated stepwise with the mean heating rate of 1 °C/min. Both samples were annealed for 0.5 h when the annealing temperature of 160 °C was reached. The SAXS patterns for the two samples are shown in Figure 8a. A considerable difference was observed between the two cases. The sample heated slowly has the structure similar to that which could be obtained for the sample annealed at lower temperature (80–120 °C, cf. Figure 5). This means that in the sample heated slowly the relaxed equilibrium state of morphology has been reached close to the temperature of glass transition.

It was observed that variation of the cooling rate of samples after annealing does not remarkably influence the structure.

8. Effect of Initial Deformation. Figure 8b shows a series of SAXS patterns recorded for samples of TR 41-1648 annealed at 100 °C for 0.5 h but deformed initially to various draw ratios λ_0. It is seen for samples deformed above the yield point that the structure after annealing at the specified conditions is almost the same and independent of the draw ratio.

IV. Molecular Interpretations on Observed Morphological Changes

To discuss the results presented in section III on a molecular level we have to first refer to the initial deformed state. As was already briefly described, the cylindrical polystyrene domains are preferentially oriented at directions inclined by small angles (the angle α in Figures 2 and 6a) to the deformation direction, and their interdomain distances are correlated along the deformation direction (i.e., **r** ∥ SD in Figure 6a). This suggests that the polybutadiene parts of molecules are highly stretched along the deformation direction and their end-to-end vectors in the deformed state determine the correlation of distances between neighboring PS domains (Figure 6a).

Relative positions of molecules in such stretched systems at room temperature are fixed because their ends (PS blocks or chemical junctions between PS and PB) are fixed in the glassy polystyrene domains. If the glassy PS domains are preserved, even under high external stresses the sample deformed to high extension can recover to almost

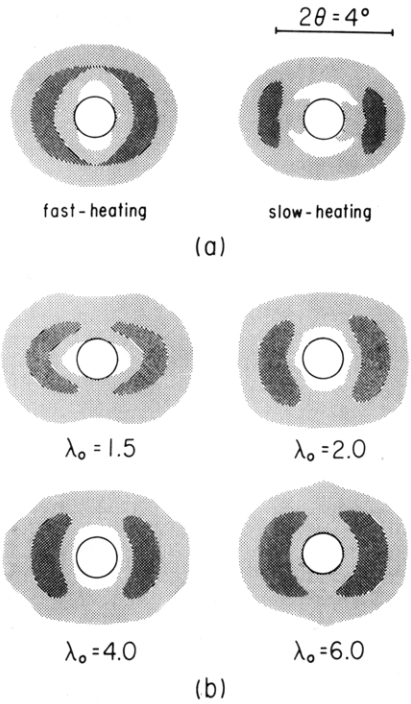

Figure 8. (a) Comparison of SAXS patterns for the samples annealed after fast heating and slow heating to the annealing temperature. (b) Comparison of SAXS patterns of the annealed samples drawn initially to various draw ratios indicated by the figures below the patterns, annealed at 100 °C.

original length and to almost randomly oriented morphological state when the external stress is removed. This "memory effect" naturally arises from the frozen-in molecular motion of polystyrene blocks in the glassy domains and shows that the plastic flow in polystyrene domains which could lead to nonrecoverable displacements of polystyrene block is very limited when the deformation and the annealing is performed at room temperature.

Experimental results presented in this paper show that when the highly deformed sample is annealed at higher temperatures the stress applied to the sample is relaxed and the microdomain structure undergoes the nonrecoverable rearrangements (as shown schematically in Figure 6, part d or part d′) in which the microdomain structure is preserved but the cylindrical domains of polystyrene become oriented along the direction of sample deformation (**n**′ ∥ SD and **r**′ ⊥ SD as in Figure 6d′). An interpretation of these results has to take into account that the relaxation of stresses in the sample has to be related to the decrease of extension of elastically stretchable PB parts of molecules, the "bridge" molecules interconnecting the neighboring PS domains. This contraction of the end-to-end vector of the bridge molecule inevitably leads to changes of relative positions of PS end blocks (Figure 9b).

The displacements of PS end blocks comprising the glassy PS domains are hindered by both (i) the presence of the interface between the two coexisting microphases and (ii) the potential barrier built up by intermolecular interactions inside the glassy PS phase. Displacement of the former type (i) involves the displacement of the end blocks across the interface, involving pulling out the end blocks, mixing them with PB matrix, and reentering them into PS microdomains. The displacements must overcome the potential barrier related to the heat of mixing of PS and PB blocks. The barrier determines the positional stability of the PS blocks across the interface. In contrast, displacement of the latter type (ii) involves displacement of the end blocks within their own microdomains. The

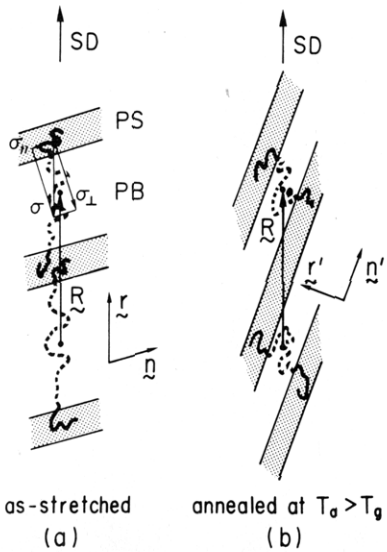

Figure 9. Schematic representation of thermally induced structural reorganization invoked by relaxation of polybutadiene chain orientation and flow of PS chains. The reorganization is characterized by the changes $\mathbf{r} \rightarrow \mathbf{r}'$ and $\mathbf{n} \rightarrow \mathbf{n}'$: (a) as-stretched, (b) after annealing at $T_a > T_g$. Note that the vector connecting the center of the bridge polybutadiene chains **R** is essentially constant and parallel to SD before and after the annealing.

latter displacement must overcome the barrier responsible for the plastic flow of polystyrene. The positional stability of the end blocks within their own microdomains is determined by the intermolecular forces.

In displacement of the latter case both PS and PB blocks interconnected by the chemical junction will move only inside their own microdomains, involving a lateral displacement of the chemical junction points of the block polymer molecules along the interface. Displacement of the former type will lead to local disruption of the interface between the two phases and to molecular mixing of PS and PB blocks. For the molecular rearrangement related to the movement of polystyrene blocks parallel to the interface the height of the barrier is determined by the free-energy barrier of plastic flow inside the PS phase.

$$\Delta F_{\parallel} = \Delta F_{\text{flow}} \tag{1}$$

For the molecular rearrangement that involves the movement of PS blocks across the interface the barrier is higher because of the contribution of the free energy of mixing ΔF_{mix}.

$$\Delta F_{\perp} = \Delta F_{\text{flow}} + \Delta F_{\text{mix}} \tag{2}$$

In the stressed system the effective heights of barriers are modified by the mechanical energy stored in the system and can be considerably depressed along directions that lead to relaxation of stresses. In such cases the local thermal fluctuation ΔW required for the activation of the molecular rearrangement becomes smaller than in the unstressed system and is related to the free enthalpy barrier ΔG. For the two types of rearrangements considered here, "parallel" and "perpendicular" to the interface, the thermal activation will occur when

$$\Delta W > \Delta G_{\parallel} = \Delta F_{\parallel} - E_{\parallel} \tag{3}$$

or when

$$\Delta W > \Delta G_{\perp} = \Delta F_{\perp} - E_{\perp} \tag{4}$$

where $E_{\parallel}$ and $E_{\perp}$ are the mechanical energy contributions related to the stress components $\sigma_{\parallel}$ and $\sigma_{\perp}$ parallel and perpendicular to the interface, respectively, (Figure 9a). E and σ are related by

$$E = \sigma V \Delta\epsilon \tag{5}$$

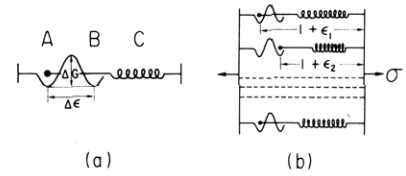

Figure 10. Model to describe the mechanical and birefringence behavior of drawn and annealed block polymer samples: (a) single model element, (b) parallelly connected assembly of the elements.

where V is the activation volume and $\Delta\epsilon$ is the extension. Both are related to the local rearrangement. It is obvious that the system will relax by the rearrangements for which the necessary thermal energy fluctuation is the smallest. The inequality

$$\Delta G_{\parallel} < \Delta G_{\perp} \tag{6}$$

which by consideration of eq 1–4 leads to

$$E_{\perp} - E_{\parallel} < \Delta F_{\text{mix}} \tag{7}$$

describes a condition of preferential occurrence of displacements of the PS block inside the PS domain without crossing the interface, i.e., the condition for structural changes with preservation of the microdomain identity, as observed in the results presented in the experimental part of this paper. It shows that the initial orientation of polystyrene microdomains with respect to the externally applied stress plays an important role in the type of structural changes observed, as it determines the difference between $E_{\perp}$ and $E_{\parallel}$.

When one considers the initial orientation of PS microdomains in the stretched sample as well as displacements of polystyrene blocks only inside their own microdomains, i.e., parallel to the interface, the structural rearrangement associated with relaxation of stretched PB block chains and with rotation of the cylindrical polystyrene domains can be illustrated schematically, as shown in Figure 9. This type of rearrangement can be related to the transition from case a to case d in Figure 6. In such rearrangement the relative positions of the two polybutadiene block chains, as described by the displacement vector **R** between their centers of gravity (denoted in Figure 9 by **R** connecting the two black points and orienting along the stretching direction), can remain almost constant, so the rearrangement can undergo homogeneously in the whole sample without the changes of the sample length found in the experimental results. The annealing causes the structural rearrangements, as specified by the change of orientations of **r** and **n** into **r**′ and **n**′ under the constraint of **R** being nearly constant. The rearrangements involve orientation relaxation of polybutadiene chains and lateral flow of the chemical junctions.

V. Two-State Model To Describe Anomalous Behavior of Birefringence as a Function of T_a

Taking the above considerations into account, we can suggest a kind of phenomenological model that can qualitatively predict the changes taking place in samples upon annealing. An element of such a model is illustrated in Figure 10a. It consists of a spring (C) representing the entropy elasticity of polybutadiene block chain. The deformation of the spring is related to deformation and orientational changes in polybutadiene phase. One end of the spring can assume two metastable states, A and B, which are related to two different relative positions of PS blocks, corresponding to before and after the plastic flow of the polystyrene end blocks in externally relaxed states, respectively. The states A and B are separated by a barrier

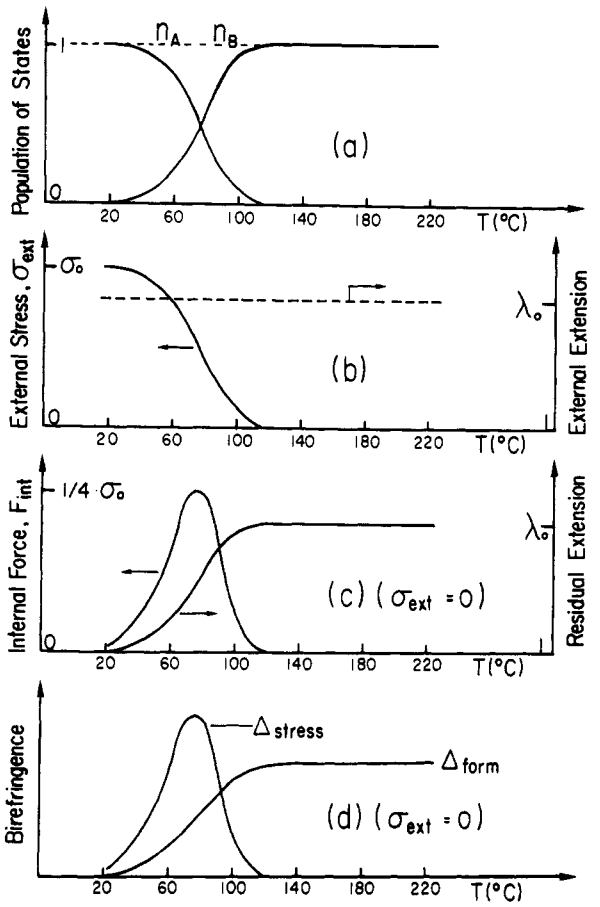

Figure 11. Temperature dependences of the characteristic parameters of the model: (a) population of states A (n_A) and B (n_B) in the model; (b) residual external stress (σ_{ext}) and extension (λ_0) for the extended state of the model; (c) internal force (F_{int}) and residual draw ratio (λ) for the relaxed state of the model; (d) schematic representation of birefringence contributions related to the internal stress (Δ_{stress}) and to the form birefringence (Δ_{form}) arising from the microdomain orientation.

ΔG that can be overcome by a thermal excitation and by an action of sufficiently high stress. The transition from A to B is accompanied by a nonrecoverable local displacement $\Delta\epsilon$, while the extension of the spring is fully recoverable. A model whose properties we would like to discuss consists of a number of such elements connected in parallel with respect to external stress (as shown in Figure 11b).

The properties of the model elements are described by identical spring constant $1/C$ and by identical heights of barriers $\Delta F = \Delta F_{flow}$. We assume that in the initial state all elements of the model are in state A, i.e., in the state of elastically deformed and oriented microdomain structure. The stress applied to such a model will involve the elastic and recoverable deformation and the nonrecoverable deformation related to jumps from state A to state B, the probability of which can be given by

$$K_{AB} = K \exp(-\Delta G_{\parallel}/kT) \tag{8}$$

The behavior of such a model in the stressed state with applied thermal energy can be easily predicted. For the initially extended model kept at constant length (λ_0) the kinetics of transition from A to B can be described by

$$dn_A/dt = -K_{AB}n_A \tag{9}$$

$$n_B = 1 - n_A \tag{10}$$

which under the condition of constant temperature lead to the solution

$$n_A = \exp(-K_{AB}t) \tag{11}$$

The population of states A and B was calculated as a function of temperature for a limited period of time and for numerical values of $\Delta G_{\parallel} = 50kT_0$, $T_0 = 300$ K, and $Kt = 2 \times 10^{18}$. Plots of n_A and n_B are shown in Figure 11a. The populations of states having been determined we can calculate changes of stress and extension of the model both in extended and in externally relaxed state. Under external extension (λ_0) the stress in the model will relax proportionally to the population of state A

$$\sigma = \sigma_0 n_A \tag{12}$$

as shown in Figure 11b. If the externally applied extension is relaxed after the heat treatment, the system can relax elastically to some residual extension λ. In such a case the condition of lack of external forces can be given by

$$n_A\sigma_1 + n_B\sigma_2 = 0 \tag{13}$$

where σ_1 and σ_2 are stresses on model elements in positions A and B, respectively. The condition of equal elongation of all model elements is (see Figure 10)

$$\epsilon_1 = \epsilon_2 + \Delta\epsilon \tag{14}$$

which, by consideration of elasticity of springs, can be written as

$$\sigma_1 C = \sigma_2 C + \Delta\epsilon \tag{15}$$

From eq 13 and 15 we can determine stresses σ_1 and σ_2 on a single spring in positions A and B, respectively, as

$$\sigma_1 = n_B\Delta\epsilon/C \qquad \sigma_2 = -n_A\Delta\epsilon/C \tag{16}$$

These equations show that for the externally relaxed model the springs in position A are under tension while those in position B are under compression. The overall extensional internal force in the model can be expressed as

$$F_{int} = n_A\sigma_1 = \Delta\epsilon n_A(1 - n_A)/C = \sigma_0 n_A(1 - n_A) \tag{17}$$

and the residual extension of the model as

$$\lambda = 1 + \epsilon_1 = 1 + \sigma_1 C = 1 + n_B\Delta\epsilon \tag{18}$$

The temperature dependence of F_{int} and λ, calculated by considering changes of n_A and n_B in eq 17 and 18, is shown in Figure 11c.

It is seen that the residual extension (λ), being proportional to the population of the state B (n_B), becomes equal to λ_0 at temperatures above which the transition of the model from state A to state B occurs, while the internal extensional force, being a parabolic function of n_A, has a maximum in the range of temperatures related to the transition. The internal force disappears at $n_A = 1$ and $n_A = 0$, i.e., when all elements in the model assume only one of the two possible states.

If we relate the transition from A to B to the structural rearrangements taking place in the block polymer in the vicinity of its glass transition of PS (illustrated in Figures 5 and 6), the experimentally observed temperature dependence of residual extension of samples (Figure 3) can be compared to the temperature dependence of λ predicted by the model. The comparison shows a good qualitative agreement.

Further comparison of the model with experimental results will consider internal stresses predicted in the model and the experimentally determined temperature dependences of residual birefringence. Internal stresses in externally relaxed states of samples cannot be directly observed but we can suppose that the presence of the extensional internal stress can be related to nonrelaxed

orientation of polybutadiene blocks and, consequently, to orientational birefringence. In such a case the birefringence will be maximum at temperatures where the maximum of the internal stresses is attained. In contrast, state B of the model is regarded as invoking orientation of the microdomain as depicted in Figure 9b, suggesting that the transition to state B can be related to an increase of the form birefringence: the greater the number of elements that pass from state A to state B, the greater can be the contribution of the form birefringence. Temperature dependences of the two contributions of the birefringence are plotted schematically in Figure 11d under the assumption that the orientational birefringence (Δ_{stress}) related to internally nonrelaxed extension of the model elements is proportional to the internal forces and that the form birefringence (Δ_{form}) is proportional to the number of elements that are transformed to state B. A comparison of this plot with the measured dependence of residual birefringence vs. temperature (Figure 4) suggests that the maximum of the birefringence observed below the glass transition temperature can be related to the nonrelaxed orientation of polybutadiene block chains, while the birefringence above the glass transition may be supported mainly by the form birefringence of the oriented microdomain structure.

VI. Concluding Remarks

Morphological change and structural and molecular relaxations induced by heat treatment of a highly deformed SBS block polymer in its deformed state (fixed external dimensions) were systematically studied to gain molecular understandings of deformation and relaxation mechanisms of the microdomain systems and to gain fundamental information to control domain orientation. Observed changes of microdomain morphology, elongation of bulk specimens, and birefringence with annealing temperature T_a were interpreted on the basis of two fundamental molecular processes: (a) elastic recovery of stretched PB chains whose ends are fixed in the PS domains and (b) flow (nonrecoverable displacements) of PS block chains parallel to the interface (or within the PS domains) or across the interface.

The relative contributions of the two processes depend on the rigidity of PS domains under applied external force and therefore on T_a. At low annealing temperatures such as $T_a \ll T_g$ (glass transition temperature of PS), the former contribution is dominant. The relative positions of PB molecules are fixed because their ends are firmly fixed in the glassy PS domains, giving rise to a "memory effect" such that the sample deformed to high extensions can recover to the original dimensions and the initial morphological state before deformation. As T_a goes up, the former contribution decreases and the latter contribution increases, giving rise to partially nonrecoverable deformation and the anomalous behavior of birefringence with T_a, as observed by the large birefringence maximum (at about 70 °C, as shown in Figure 4). This anomalous behavior is primarily associated with orientation of PB chains and is interpreted with the "two-state" model. At $T_a > T_g$, the latter contribution is dominant, giving rise to completely nonrecoverable deformation ($\lambda_0 = \lambda$). The memory effect is lost by the flow of PS through the nonrecoverable displacements of chemical junctions between PS and PB block chains which are expected to occur preferentially parallel to the interface, resulting in reorganization into new morphology, as shown in Figure 6d or 6d′, though the cylindrical microdomain in structure is preserved. In the newly built-up organization, the stretched PB chains are relaxed, and the microdomains change orientation toward extension direction (SD) and have positional correlation perpendicular to SD, as shown in Figure 9. In this regime the net birefringence is primarily determined by the form birefringence.

At even higher temperature $T_a > T_c$ (the order–disorder transition temperature), the memory of original microdomain structure itself is entirely lost through the dissolution process (as described in section III. 5), and new microdomain structure with microscopically random orientation is re-formed from the relaxed disordered state of block polymers when the sample is cooled below T_c. The birefringence method turned out to be a useful and quick method in studies of the order–disorder transition of some classes of block polymers.

Acknowledgment. We are grateful to Prof. H. Kawai and M. Kryszewski for their encouragements on this work. T.P. is very grateful to the Japan Society of Promotion of Sciences for the fellowship in Japan which made it possible to perform this study.

Registry No. (Styrene)·(butadiene) (copolymer), 9003-55-8.

References and Notes

(1) Akovali, G.; Niinomi, M.; Diamant, J.; Shen, M. *Polym. Prepr. (Am. Chem. Soc., Div. Polym.* Chem.) **1976**, *17*, 560.
(2) Hong, S. D.; Shen, M.; Russell, T.; Stein, R. S. in "Polymer Alloys"; Klempner, D.; Frisch, K. C.; Eds.; Plenum Press: New York, 1977.
(3) Fujimura, M.; Hashimoto, T.; Kawai, H. *Rubber Chem. Technol.* **1978**, *51*, 215.
(4) Hashimoto, T.; Fujimura, M.; Saijo, K.; Kawai, H.; Diamant, J.; Shen, M., *Adv. Chem. Ser.* **1979**, *176*, 257.
(5) Kotaka, T.; Miki, T.; Arai, K. *J. Macromol. Sci., Phys.* **1980**, *17*(2), 303.
(6) Pakuła, T.; Saijo, K.; Kawai, H.; Hashimoto, T. *Macromolecules* **1985**, *18*, 1294.
(7) Fujimura, M.; Hashimoto, H.; Mori, K.; Hashimoto, T. Unpublished data.
(8) Hashimoto, T.; Suehiro, S.; Shibayama, M.; Saijo, K.; Kawai, H. *Polym. J.* **1981**, *13*, 501.
(9) Fujimura, M.; Hashimoto, T.; Kawai, H. *Mem. Fac. Eng., Kyoto Univ.* **1981**, *43*, 224.
(10) Wiener, O. *Abh. Saechs, Akad. Wiss. Math. Phys.* **1912**, *32*, 507.
(11) Leibler, L. *Macromolecules* **1980**, *13*, 1602.
(12) Noolandi, J.; Hong, K. M. *Ferroeletrics* **1980**, *30*, 117.
(13) Hashimoto, T.; Shibayama, M.; Kawai, H. *Polym. Prepr. (Am. Chem. Soc., Div. Polym. Chem.)* **1982**, *23*(1), 21. *Macromolecules* **1983**, *16*, 1093.
(14) Hashimoto, T.; Kowsaka, K.; Shibayama, M.; Kawai, H. *Polym. Prepr. (Am. Chem. Soc., Div. Polym. Chem.)* **1983**, *24*(2), 224.
(15) Zin, W.-C.; Roe, R.-J. *Macromolecules* **1984**, *17*, 183.
(16) See, for example, Haken, H. "Synergetics; An Introduction, Nonequilibrium Phase Transitions and Self-Organization in Physics, Chemistry and Biology"; Springer-Verlag: Heidelberg, 1978.
(17) Mori, K.; Hasegawa, H.; Hashimoto, T. *Polym. J.* **1985**, *17*, 799.